The following supplement accompanies the article

The paradox of inverted biomass pyramids in kelp forest fish communities

Rowan Trebilco[1,2*], Nicholas K. Dulvy[1], Sean C. Anderson[1], & Anne K. Salomon[3]

[1]Earth to Ocean Research Group, Biological Sciences, Simon Fraser University, 8888 University Drive, Burnaby, BC, Canada V5A 1S6

[2]Antarctic Climate and Ecosystems Cooperative Research Centre, University of Tasmania, Private Bag 80, Hobart, TAS 7001 Australia

[3]School of Resource and Environmental Management, Simon Fraser University, 8888 University Drive, Burnaby, BC, Canada V5A 1S6

[*] *Corresponding author email:* rtrebilc@sfu.ca

Supplimentary materials for methods

Study area

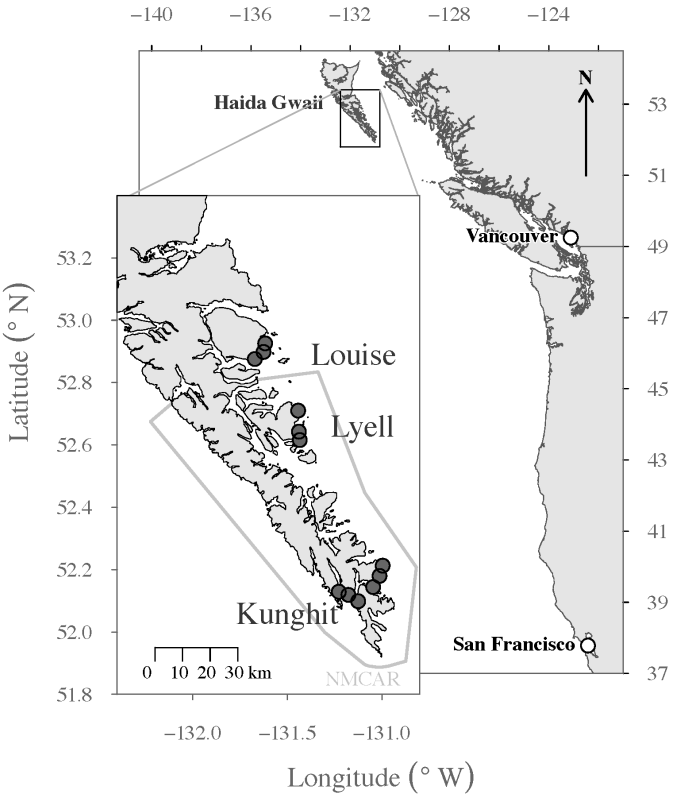

Figure S1: Study sites (points) were located on the southern shores of Haida Gwaii (formely the Queen Charlotte Islands) off the northwest coast of British Columbia, Canada. The boundaries of the Gwaii Haanas National Marine Conservation Area Reserve (NMCAR) and Haida Heritage Site are shown in light gray.

Survey methods

Surveys were undertaken in the summer (between late June and early August) each year from 2009 to 2012, with the majority of sites surveyed every year, yielding a total of 37 unique combinations of site and year in the dataset (a full summary of survey protocol is provided in [1]). Four to six 30 m long by 4 m wide belt transects were surveyed at each site in each year (four at each site in 2009, six at each site in 2010, 2011 and 2012), split evenly between 'deep' and 'shallow' strata (tide-corrected depth of 12.0 ± 1.3 m and 7.7 ± 1.1 m below chart datum respectively). Transects were

deployed parallel to shore, with the ends of each transect separated by a minimum of 5 m. For each transect an individual diver deployed a plastic transect meter tape while swimming forward at an approximately constant speed [2], recording conspicuous fishes present in the sampling area (all fishes other than blennies, gobies, gunnels and other small cryptic species, table S1). Count time was not standardised as it was dependent on fish abundance and habitat characteristics.

Sample processing and stable isotope analysis

In the laboratory, white muscle tissue samples were thawed, rinsed with 10% HCl followed by de-ionised water, and oven dried for 48 hours at 60°C. Samples were then manually ground to a fine powder and 1 ± 0.2 mg portions were packaged into 5 x 3.5 mm tin capsules. δ^{13}C and δ^{15}N values for packaged samples were measured using a PDZ Europa ANCA-GSL elemental analyzer interfaced to a PDZ Europa 20–20 isotope ratio mass spectrometer. δ^{13}C and δ^{15}N were calculated as:

$\delta^{15}X = \left(\frac{R_{\text{sample}}}{R_{\text{standard}}} - 1\right) \times 1000$

where R_{sample} and R_{standard} are the ratio of heavy:light isotopes (^{13}C:^{12}C and ^{15}N:^{14}N) in the sample and the international standard (V-PBD for C and air for N) respectively. δ units are parts per thousand (‰). Stable isotope analyses were conducted by the UC Davis Stable Isotope Facility (SIF).

In this study we implicitly assumed that a shared isotopic baseline for δ^{15}N was representative of all fish sampled. This assumption was supported by the observation of a mean δ^{15}N of 10.32 (n = 47, s.d. = 0.4) for rock scallops (*Crassodoma gigantea*) that were opportunistically collected at the same sites where fish were sampled (placing them one trophic level below the smallest fish sampled). Because they are among the longest-lived filter-feeding invertebrates present on the reefs of Haida Gwaii, rock scallops provide a time-integrated baseline estimate for δ^{15}N for this system.

Zero-handling in biomass spectrum fits

In this manuscript we follow the precedent in the literature of treating size classes in which no biomass was observed as empty rather than as zeros in fitting biomass spectra. In order to determine whether our conclusions were sensitive to this decision we fit a second model in which we populated empty bins for a given location/year with a biomass equal to half the minimum of the biomass observed in that bin across other locations/years. Doing so resulted in a decreased slope estimate (0.33, 95% CIs 0.03–0.62) but does not affect our conclusions.

Bayesian hierarchical approach to estimate community predator-to-prey mass ratio

We used a Bayesian hierarchical approach to model the community relationship between trophic position and body-size, and estimated the community mean PPMR from the posterior distribution of slopes of this relationship. Our calculation of PPMR from the slope of the community relationship between trophic position and body-size followed [3]. Adopting a Bayesian hierarchical approach allowed us to account for the nested nature of the data (species sampled within locations) and to explicitly incorporate important sources of uncertainty, including instrument error in measurements of δ^{15}N and uncertainty in the assumed rate of δ^{15}N fractionation (Δ^{15}N) with increasing trophic position.

Preliminary exploratory analyses fitting models with the R package `lme4`, and not accounting for measurement error, indicated that a random-effect structure allowing slope to vary randomly with species and an intercept to vary randomly with species and area was best supported by the data (lowest AIC). We retained this random-effect structure in the Bayesian model that we describe below. These preliminary analyses also indicated minimal correlation between random slopes and intercepts. Therefore, for simplicity, we proceeded with a Bayesian hierarchical model that did not model correlation between random effects.

To build our model, we first assigned each individual fish for which $\delta^{15}\mathrm{N}$ was measured into $\log_2$ body mass classes ($\log_2 \mathrm{M}$). We centered the $\log_2 \mathrm{M}$ predictor by subtracting the mean to reduce correlation between random effect intercepts and slopes then modeled $\delta^{15}\mathrm{N}$ as (with $\mathcal{N}$ denoting normal distributions, σ and τ denoting standard deviations about the means):

$\delta^{15}\mathrm{N}_i^{\mathrm{true}} = \alpha + \alpha_j + \alpha_k + (\beta + \beta_j) \cdot \log_2 \mathrm{M}_i + \epsilon_i,$

For $i = 1, \ldots, N$ observations, $\quad j = 1, \ldots, J$ species, $\quad k = 1, \ldots, K$ locations,

$\alpha_j \sim \mathcal{N}(0, \sigma_\alpha^2), \quad \beta_j \sim \mathcal{N}(0, \sigma_\beta^2), \quad \alpha_k \sim \mathcal{N}(0, \tau_\alpha^2), \quad \epsilon_i \sim \mathcal{N}(0, \sigma^2).$

We incorporated measurement error around $\delta^{15}\mathrm{N}_i^{\mathrm{true}}$ as:

$\delta^{15}\mathrm{N}_i^{\mathrm{measured}} \sim \mathcal{N}(\delta^{15}\mathrm{N}_i^{\mathrm{true}}, 0.04),$

where $\delta^{15}\mathrm{N}_i^{\mathrm{measured}}$ represents a measured value of $\delta^{15}\mathrm{N}$ and 0.04 represents the assumed measurement variance (based on personal communication from the UC Davis SIF).

We chose non-informative normal priors on $\{\alpha, \alpha_j, \alpha_k, \beta, \beta_j\} \sim \mathcal{N}(0, 10^6)$, a uniform prior U(0, 100) on the residual standard deviation σ, and weakly informative half-Cauchy priors with scale parameters of 10 on the standard deviation parameters $\sigma_\alpha, \sigma_\beta$ and τ_α to constrain the parameter to reasonable values and aid computation [4]. The shape the half-Cauchy priors (lines; scale parameter of 10) used on standard deviation hyperparameters is shown below overlain on their observed posterior distributions (bars). The priors are unlikely to drive the posterior distributions of the standard deviation hyperparameters as they allow for far greater values than the data suggest, while somewhat limiting extreme values and thereby aiding computation:

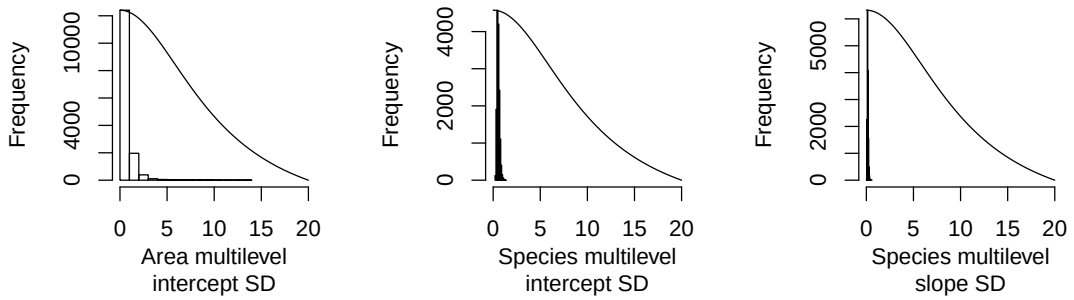

We then estimated PPMR incorporating uncertainty in fractionation rate ($\Delta^{15}\mathrm{N}$) as:

$$\text{PPMR} = 2^{\Delta^{15}\text{N}/\beta}, \quad \Delta^{15}\text{N} \sim \mathcal{N}(\mu_{\Delta^{15}\text{N}}, \sigma^2_{\Delta^{15}\text{N}}).$$

We assumed a mean fractionation ($\mu_{\Delta^{15}\text{N}}$) of 3.2 ‰ with a standard deviation ($\sigma_{\Delta^{15}\text{N}}$) of 1. 3.2 ‰ has been recommended as an assumed value for fish white muscle tissue [5], and adding a wide standard deviation around this assumed mean encompasses the other widely recommended value of 3.4 ‰ [6, 7] as well as making our PPMR estimate robust to emerging evidence that fractionation rate may vary with body-size and species (although such variation is likely to be small within the range of body-sizes considered here; [8, 9]).

We drew samples from the posterior distribution of all parameters using `JAGS` [10]. We ran 100,000 iterations with three chains, discarded the first 50,000 iterations as burn in, and recorded every 10^{th} iteration value thereafter for a total of 15,000 posterior samples. We assessed chain convergence with the Gelman-Rubin diagnostic (all were below 1.1) and visual inspection of the chains [11] and performed graphical posterior predictive checks (as shown below) to ensure our probability model could recreate similar data [11]. These show realizations of the parameter vector θ from the posterior samples. The left panel corresponds to the observed data and the two panels to the right correspond to replicated datasets simulated from the model. The colours represent different species. The replicated datasets y^{rep} resemble our original dataset y and we do not observe systematic differences in the datasets:

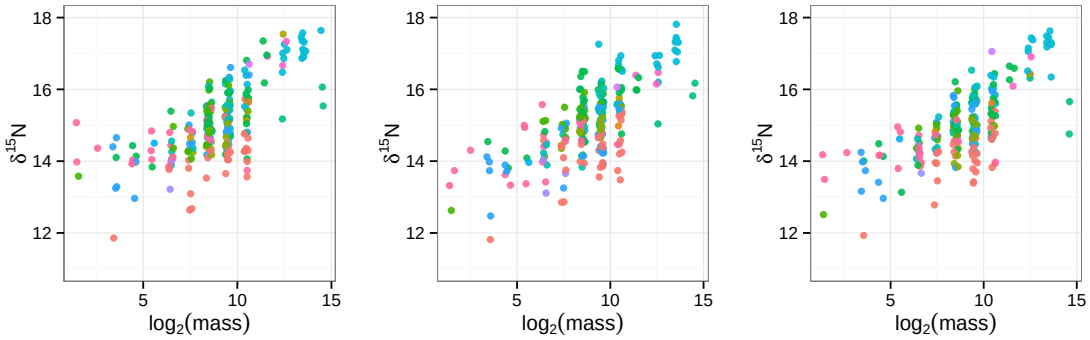

We also examined the residuals from two example MCMC draws arranged along the the predictor ($\log_2 \text{M}$) and shown by species (with colour for area):

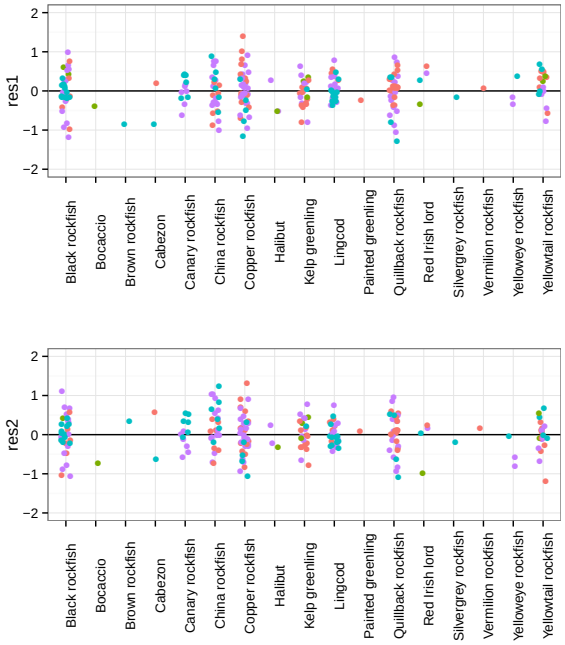

106 And by area (with colour for species):

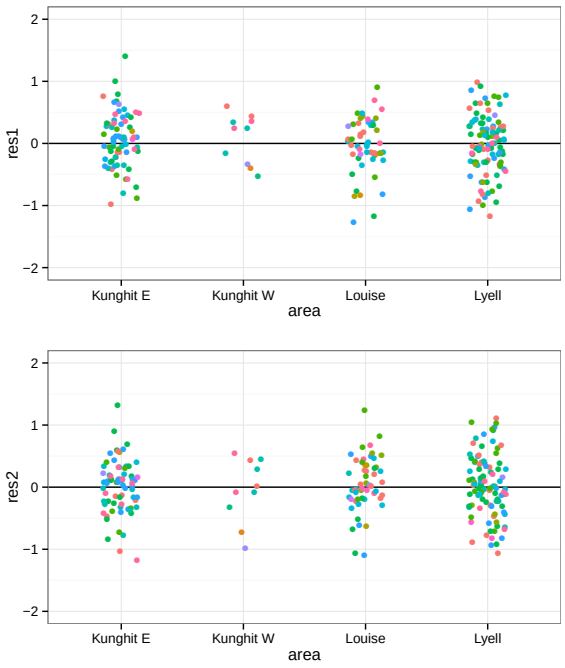

The lack of structure of the residuals in both representations indicates that there is not systematic unaccounted-for variation associated with either location or species that may be biasing the models.

We performed a jackknife procedure to evaluate sensitivity of estimated PPMR to the individual species included in the analysis. For each jackknife we ran 10,000 model iterations with 3 chains, discarding the first 5000 as burn-in and keeping every 5^{th} iteration value thereafter for a total of 3000 saved samples per jackknife.

The `JAGS` code for the model was:

```
model {
  # Priors
  b0 ~ dnorm(0, 1.0E-6) # intercept
  b1 ~ dnorm(0, 1.0E-6) # slope
  sigma_res ~ dunif(0, 100) # residual SD

  # weakly informative priors (Gelman 2006)
  # half-Cauchy with scale parameter of 10
  sp_b0_sd ~ dt(0, 1/(10*10), 1) T(0, ) # species intercept multilevel SD
  sp_b1_sd ~ dt(0, 1/(10*10), 1) T(0, ) # species slope multilevel SD
  ar_b0_sd ~ dt(0, 1/(10*10), 1) T(0, ) # location intercept multilevel SD

  # Transformations from variance to precision
```

```
  tau_res <- pow(sigma_res, -2)
  frac_tau <- pow(frac_sd, -2)
  sp_b0_tau <- pow(sp_b0_sd, -2)
  sp_b1_tau <- pow(sp_b1_sd, -2)
  ar_b0_tau <- pow(ar_b0_sd, -2)
  d15N_tau <- pow(d15N_sd, -2)

  # Multilevel effects for species
  for (j in 1:N_sp) {
    sp_b0[j] ~ dnorm(0, sp_b0_tau) # intercepts
    sp_b1[j] ~ dnorm(0, sp_b1_tau) # slopes
  }

  # Multilevel effects for location
  for (k in 1:N_ar) {
    ar_b0[k] ~ dnorm(0, ar_b0_tau) # intercepts
  }

  # Likelihood data model
  for (i in 1:N) {
    y_hat[i] <- b0 + sp_b0[sp[i]] + ar_b0[location[i]] +
      (b1 + sp_b1[sp[i]]) * log_m[i] # predicted delta 15 N
    obs_delta[i] ~ dnorm(delta[i], d15N_tau) # measurement error on d15N
    delta[i] ~ dnorm(y_hat[i], tau_res) # likelihood model
  }

  # Derived values
  frac ~ dnorm(frac_mu, frac_tau) # fractionation rate with error
  ppmr_exponent <- frac / b1 # exponent in PPMR equation

  # Predictions at location random effect of zero
  for (i in 1:N) {
    y_hat2[i] <- b0 + sp_b0[sp[i]] +
      (b1 + sp_b1[sp[i]]) * log_m[i] # predicted delta 15 N
  }

  # Fixed effect predictions at smoothed set of log_m
  for (h in 1:N_pred) {
    y_hat3[h] <- b0 + b1 * log_m_pred[h] # predicted delta 15 N at smoothed log_m
  }
}
```

Biomass-weighted hierarchical linear model for the estimation of community PPMR

We also evaluated a biomass-weighted hierarchical linear model to estimate community PPMR. Using visual survey data, we calculated the proportion of the total observed biomass in each size bin contributed by each species in each location (with biomass from all survey observations summed within locations). These proportions were then matched to isotope samples based on the species from which it was obtained, its mass, and the location where it was sampled, and included as weightings in a hierarchical linear model for the relationship between trophic position and individual body mass, fit using the R package `lme4` [12]. Not all species for which isotope samples were obtained were observed on visual surveys. Further, not all species that were observed on surveys were observed at all sizes in all locations. Therefore, we used the following decision rules to assign missing weightings:

1. If a species was not observed on visual surveys for a given $\log_2$ size-class in one location, but was observed in that size-class in other locations, isotope samples for the size-class/location combinations where it was not observed were assigned the mean weighting for that size-class from those locations where it was observed.

2. If a species was not observed in a given $\log_2$ size-class in any location, isotope samples for that species/size-class were assigned a weighting of half of the lowest weighting from all other species observed in that size-class and location.

3. If no fish of any species were observed in a $\log_2$ size-class in any location, samples were assigned a weighting of 0.5

Using these weightings, we modeled biomass spectra as hierarchical linear regression with $\log_2(\mathrm{M})$ as the predictor and $\log_2 \delta^{15}\mathrm{N}$ as the response. The spatially nested sampling design was accounted for by allowing intercept to vary randomly with location. Slope and intercept were allowed to vary randomly by species. PPMR was calculated from the global regression slope (β) as $\mathrm{PPMR} = 2^{\Delta^{15}\mathrm{N}/\beta}$ assuming a fractionation rate ($\Delta^{15}\mathrm{N}$) of 3.2 ‰.

We recognise that our Bayesian methodology is potentially susceptible to bias since the data were not weighted by their proportional contribution to total community biomass. However, the fact that we obtained an almost identical PPMR estimate (5861) using a biomass weighted hierarchical linear model gives confidence that the PPMR estimate we obtained from the Bayesian model accurately reflects the true community PPMR. The insensitivity of the PPMR estimate to species weightings is a result of the fact that species-level slopes for the relationship between trophic position and body size are all similar (and positive) in this system (figure S3). Weighting by biomass would be more important if slopes varied widely among species, as observed in the North Sea [13], and developing methods that both account for uncertainty and allow for species biomass weightings will be an important goal for future studies.

Supplementary materials for results

Species surveyed and sampled

Table S1: Species surveyed on transects and sampled for stable isotope analysis, with visually assessed stomach contents

species	n surveyed	n sampled	mass range surveyed (g)	mass range sampled (g)	prey items (no. of sampled fish for which item present in gut)			
					fish	crabs	other reef invertebrates	pelagic zooplankton
Yellowtail rockfish (*Sebastes flavidus*)	1837	20	33–495	3–1300	3	0	0	0
Black rockfish (*Sebastes melanops*)	1452	34	36–1923	10–1563	16	0	8	6
Kelp greenling (*Hexagrammos decagrammus*)	476	23	34–1950	80–1075	6	10	8	7
Copper rockfish (*Sebastes caurinus*)	245	42	38–1297	14–2400	11	15	13	9
Quillback rockfish (*Sebastes maliger*)	195	33	40–1273	9–1180	9	8	8	8
China rockfish (*Sebastes nebulosus*)	128	26	39–1050	4–884	3	15	9	1
Puget Sound rockfish (*Sebastes emphaeus*)	106	0	85–119					
Painted greenling (*Oxylebius pictus*)	32	1	43–216	40–40	0	0	1	0
Lingcod (*Ophiodon elongatus*)	26	27	208–1381	478–17900	12	0	1	1
Striped perch (*Embiotoca lateralis*)	13	0	129–678					
Vermilion rockfish (*Sebastes miniatus*)	9	1	262–883	800–800	0	0	0	0
Canary rockfish (*Sebastes pinniger*)	4	12	110–951	240–1450	0	0	0	1
Cabezon (*Scorpaenichthys marmoratus*)	4	2	1248–1862	1450–7500	0	1	1	0
Rock greenling (*Hexagrammos lagocephalus*)	3	0	355–355					
Red Irish lord (*Hemilepidotus hemilepidotus*)	3	4	49–226	90–170	1	1	2	0
Tiger rockfish (*Sebastes nigrocinctus*)	1	0	97–97					
Kelp perch (*Brachyistius frenatus*)	1	0	94–94					
Buffalo sculpin (*Enophrys bison*)	1	0	639–639		0	1	0	0
Brown Irish lord (*Hemilepidotus spinosus*)	1	0	441–441					
Yelloweye rockfish (*Sebastes ruberrimus*)	0	3		2750–6300	1	0	1	0
Silvergrey rockfish (*Sebastes brevispinus*)	0	1		1160–1160	0	0	0	0
Halibut (*Hippoglossus stenolepis*)	0	3		6800–31200	1	1	0	0
Brown rockfish (*Sebastes auriculatus*)	0	1		250–250	1	0	1	0
Bocaccio (*Sebastes paucispinis*)	0	1		1800–1800	0	0	0	0

Model results

Figure S2: Probability density plots from the jackknife analysis showing the distribution of PPMR estimates obtained, excluding one species at a time from the model. Colour coding indicates the individual species excluded in each iteration. The single line that is slightly distinct from the others represents Yellowtail rockfish.

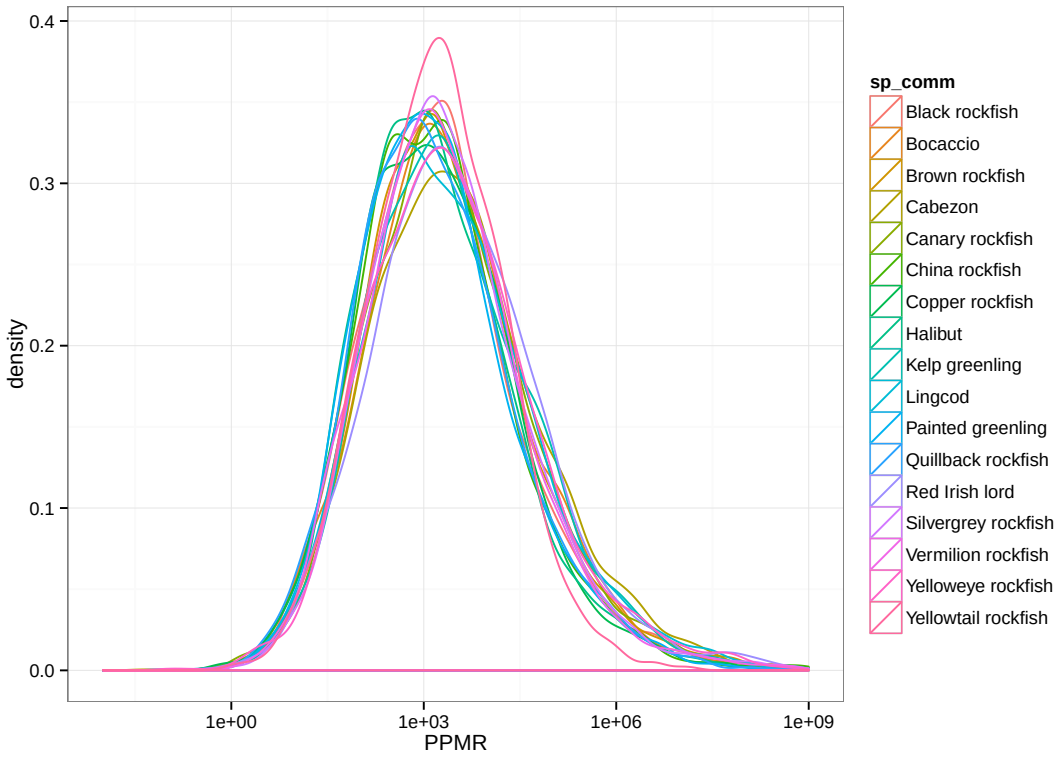

Figure S3: Species-level slope estimates from weighted hierarchical linear model fit with `lmer` vs. the non-weighted hierarchical Bayesian model fit using `JAGS` that incorporates measurement errors. The global slope estimates are shown as coloured vertical lines and are nearly the same. Area of dots is pro''portional to the weights for `lmer` model points and held constant for `JAGS` model points. Confidence intervals are +/- 1.96 random effect standard errors for `lmer` and 2.5 and 97.5 quantiles for `JAGS`. Estimates are ordered by decreasing `JAGS` estimate from top to bottom.

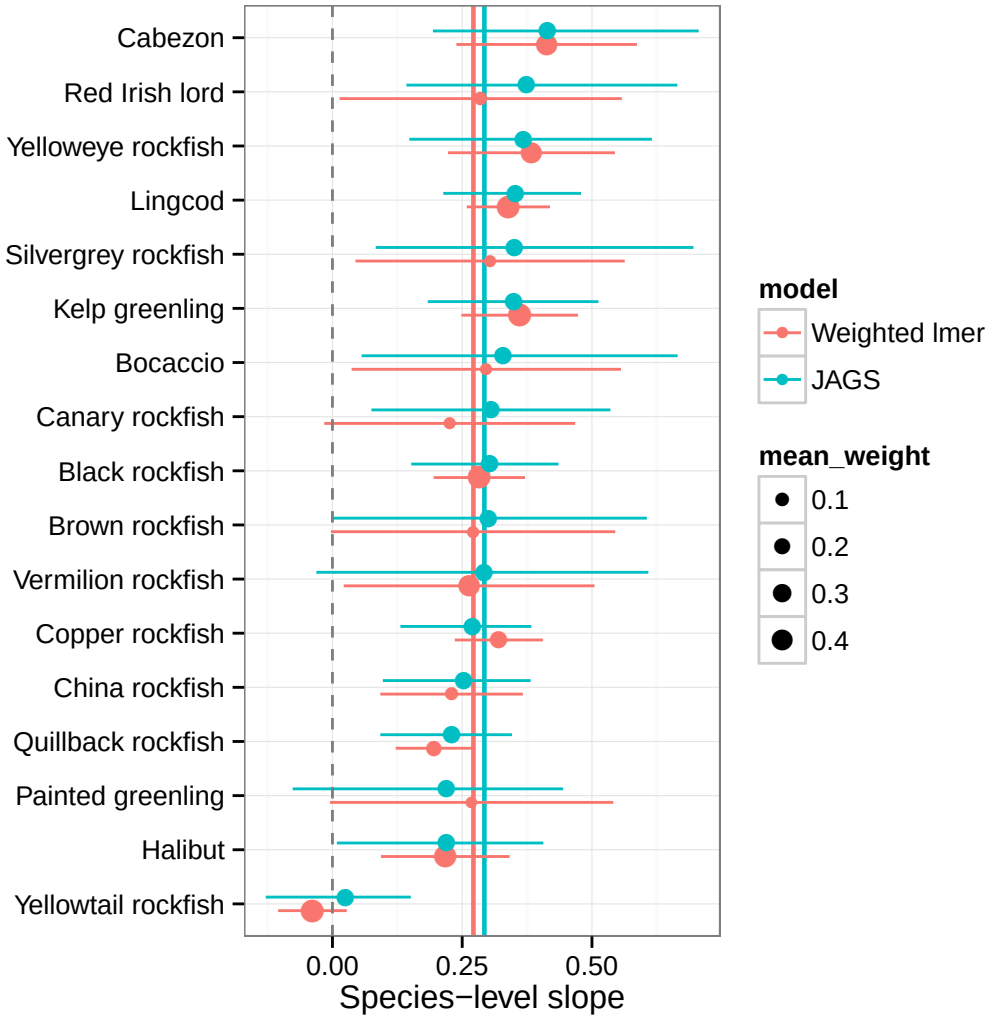

References

[1] Trebilco R, Demes KW, Lee LC, Keeling BE, Sloan NA, Stewart HL, Salomon AK, 2014 Summary of Baseline Kelp Forest Surveys Within and Adjacent to Gwaii Haanas National Park Reserve, National Marine Conservation Area Reserve and Haida Heritage Site, Haida Gwaii, British Columbia, Canada. *Can. Data Rep. Fish. Aquat. Sci.* **1252**. www.dfo-mpo.gc.ca/Library/352932.pdf

[2] Watson RA, Carlos GM, Samoilys MA, 1995 Bias introduced by the non-random movement of fish in visual transect surveys. *Ecol. Model.* **77**, 205–214

[3] Jennings S, Mackinson S, 2003 Abundance-body mass relationships in size-structured food webs. *Ecol. Lett.* **6**, 971–974

[4] Gelman A, 2006 Prior distributions on variance parameters in hierarchical models. *Bayesian Analysis* **1**, 515–533

[5] Sweeting C, Barry J, Barnes C, Polunin N, Jennings S, 2007 Effects of body size and environment on diet-tissue δ^{15}N fractionation in fishes. *J. Exp. Mar. Biol. Ecol.* **340**, 1–10

[6] Minagawa M, Wada E, 1984 Stepwise enrichment of ^{15}N along food chains: Further evidence and the relation between δ^{15}N and animal age. *Geochimica et Cosmochimica Acta* **48**, 1135–1140

[7] Post D, 2002 Using stable isotopes to estimate trophic position: models, methods, and assumptions. *Ecology* **83**, 703–718

[8] Wyatt A, Waite A, Humphries S, 2010 Variability in Isotope Discrimination Factors in Coral Reef Fishes: Implications for Diet and Food Web Reconstruction. *PLoS One* **5**, e13682

[9] Hussey NE, MacNeil MA, McMeans BC, Olin JA, Dudley SFJ, Cliff G, Wintner SP, Fennessy ST, Fisk AT, 2014 Rescaling the trophic structure of marine food webs. *Ecol. Lett.* **17**, 239–250

[10] Plummer M, 2003 JAGS: A program for analysis of Bayesian graphical models using Gibbs sampling. In *Proceedings of the 3rd International Workshop on Distributed Statistical Computing (DSC 2003).* Version 3.4.0

[11] Gelman A, Carlin JB, Stern HS, Dunson DB, Vehtari A, Rubin DB, 2014 *Bayesian Data Analysis.* Chapman & Hall

[12] Bates D, Maechler M, Bolker B, Walker S, 2013 *lme4: Linear mixed-effects models using Eigen and S4. R package version 1.0-5*

[13] Jennings S, Pinnegar J, Polunin N, Boon T, 2001 Weak cross-species relationships between body size and trophic level belie powerful size-based trophic structuring in fish communities. *J. Anim. Ecol.* **70**, 934–944